Journal of Engineering Sciences, Assiut University, Vol. 37, No. 2, pp. 393-412 , March 2009.

ROTOR RESISTANCE IDENTIFICATION FOR SPEED SENSORLESS VECTOR CONTROLLED INDUCTION MOTOR DRIVES TAKING SATURATION INTO ACCOUNT

Yehia S. Mohamed, A. M. El-Sawy and A. A. Zaki
Electrical Engineering Department, Faculty of Engineering, El-Minia University, EL-Minia, Egypt.

(Received January17, 2009 Accepted March 30, 2009)

This paper aims at developing a method of rotor resistance estimation for speed sensorless indirect vector controlled induction motor drive taking the effect of magnetic flux saturation into account. A mathematical dynamic model of an induction motor as influenced by magnetic circuit saturation is presented. Moreover, a modified structure of indirect vector controller scheme is proposed which involves the saturated value of the magnetizing inductance. In this scheme, an effective online method for rotor resistance estimation is based on a modified model reference adaptive system (MRAS) to achieve high-precise control in a wide range of motor speed. The motor speed is estimated from the difference between the estimated synchronous speed and slip speed. The online magnetizing inductance estimation algorithm to operate within the rotor resistance estimation is presented. Digital simulations have been carried out in order to evaluate the effectiveness of the proposed sensorless drive system. The results have proven excellent steady-state and dynamic performances of the drive system, which confirms validity of the proposed scheme.

LIST OF SYMBOLS

f_d	The damping coefficient of the load	L_r	Rotor self leakage inductance (H)
i_{ds}^s, i_{qs}^s	Stationary axes stator current components (A)	L_s	Stator self leakage inductance (H)
i_{ds}^e, i_{qs}^e	Synchronous axes stator current components (A)	L_{ls}	Stator leakage inductance (H)
$i_{ds}^{e\,*}, i_{qs}^{e\,*}$	Synchronous axes desired stator currents components (A)	L_{lr}	Rotor leakage inductance (H)
i_{dr}^s, i_{qr}^s	Stationary axes rotor current components (A)	$p = d/dt$	Differential operator
i_{dr}^e, i_{qr}^e	Synchronous axes rotor current components (A)	R_s	Stator resistance (Ω)
J	Moment of inertia (kg.m^2)	R_r	Rotor resistance (Ω)
L_m	Magnetizing inductance (H)	$\hat{R}_r$	Estimated rotor resistance (Ω)
$\hat{L}_m$	Estimated magnetizing inductance (H)	T_l	Load torque (Nm)

T_e	Electromagnetic torque (N.m)	θ_e	Angle between synchronous frame and stationary frame
T_r	Rotor time constant $T_r = L_r / R_r$	σ	Leakage coefficient $\left(1 - L_m^2 / L_s L_r\right)$
V_{ds}^s, V_{qs}^s	Stationary axes voltage components (V)	ω_e	Synchronous speed (rad/sec)
V_{ds}^e, V_{qs}^e	Synchronous axes voltage components (V)	ω_e^*	Command synchronous speed (rad/sec)
$\vec{\lambda}_r$	Rotor flux vector (wb)	ω_{sl}	Slip speed (rad/sec)
$\lambda_{dr}^s, \lambda_{qr}^s$	Stationary axes rotor flux components (wb)	ω_{sl}^*	Command slip speed (rad/sec)
$\lambda_{dr}^e, \lambda_{qr}^e$	Synchronous axes rotor flux components (wb)	ω_r	Actual Rotor speed (rad/sec)
$\hat{\lambda}_{dr}^s, \hat{\lambda}_{qr}^s$	Stationary axes estimated rotor flux components (wb)	ω_r^*	Reference Rotor speed (rad/sec)
$\lambda_{dm}^s, \lambda_{qm}^s$	Stationary axes magnetizing flux components (wb)	$\hat{\omega}_r$	Estimated Rotor speed (rad/sec)
λ_m	Magnitude of magnetizing flux vector (wb)		

1- INTRODUCTION

Indirect field oriented controlled induction motor drives are increasingly used in high-performance drive systems. However, in the indirect rotor flux oriented control, the rotor flux position is obtained by adding the measured rotor angle to the computed slip angle, where the latter quantity gives the position of the rotor flux relative to the direct axis of the rotor. The performance of the indirect rotor flux oriented control strongly depends on the accuracy of the slip angle which can be calculated from the reference values of the torque, the flux producing current component and rotor parameters values of the machine under consideration [7]. Therefore, in order to get the rotor position correctly, the accurate rotor circuit parameters are necessary. When incorrect parameters value is used in the controller, it may cause instantaneous errors in both torque and flux resulting in sluggish dynamics. Thus, it is essential to have accurate parameters of the machine in order to achieve the ideal instantaneous torque control. The schemes used in field orientation induction machines for rotor flux estimation and indirect vector control is derived from the constant parameter of induction machine model. However, actual machine parameters are subjected to variation due to temperature change and magnetic saturation. These parameters are rotor resistance, mutual inductance and rotor leakage inductance. As consequence, mismatch between actual parameters and parameters used in the control parts of the system occurs, leading to detuned operation of the drives. The use of speed sensor not only spoils the ruggedness and simplicity of induction motor, but also, it increases the cost and complicity of the control system.

Several methods have been reported to minimize the consequences of rotor resistance sensitivity in the indirect vector controlled induction motor drives. These methods have been discussed in [7]. The method discussed in [1]-[2] is based on model

reference adaptation of either flux or reactive power. The second approach was to compensate the rotor resistance variation by adaptive feedback linearization control with unknown rotor resistance which has been developed in [3]. The third identification method is to detect the output signal variation invoked by the artificial injection signal [4]. Also, an Extended Kalman filter was used for rotor resistance identification in [5]-[6]. All of these methods assumed that there is no change in the magnetizing inductance during the rotor resistance estimation. So the accuracy of these methods has been affected by the variation of the magnetizing inductance, if the magnetic circuit of the induction motor has been saturated.

On the other hand, to eliminate the speed sensor the rotor speed has to be estimated from measured stator voltages and currents at the motor terminals. Different speed estimation algorithms are used for this purpose and discussed in [16]-[17]. Some of these methods are based on a non-ideal phenomenon such as rotor slot harmonics. Another class of algorithms relies on some kind of probing signals injected into stator terminals (voltage and/or current) to detect the rotor flux and consequently, the motor speed. Such methods require spectrum analysis, which besides being time consuming procedures; they allow a narrow band of speed control. Alternatively, a great deal of research interest is given to speed estimation methods based on the machine model for its simplicity. These methods exhibit accurate and robust speed estimation performance; however they are highly dependent on the machine parameters [17].

In many variable torque applications, it is desirable to operate the machine under magnetic saturation to develop higher torque [12]. Also, for the vector control to operate with a wide range of speed, a reduction of the rotor flux in the speeds higher than the base speed causes the magnetizing inductance to vary nonlinearly. That affects the accuracy of the performance of the vector control scheme. Some methods have been introduced to study and compensate the magnetizing inductance variation in the vector control of the induction motor performance. Methods [8]-[9] suggest a method for tuning the magnetizing inductance but these methods used the speed sensors or were suffered from decoupling problems with the rotor speed. Another method used in [10]-[11] depends on measured stator voltages and currents and the magnetizing curve of the machine and this method is characterized with its simplicity. The saturation effect in the indirect vector control of induction motor has been investigated/compensated by various authors [13]-[14]. Previous authors [13-14] have investigated the performance of vector controlled induction motor drives as influenced by magnetic saturation and its compensation without paying attention to the influence of rotor resistance variation. Also, 1n [18], the speed sensorless of vector controlled induction motor has been presented taking saturation into account but assuming constant rotor resistance. On the other hand, no attempt has been made to investigate the effect of magnetic saturation on the performance of rotor resistance estimation for sensorless indirect vector controlled induction motor drives.

In this paper, the rotor resistance identification for a speed sensorless vector controlled induction motor drives taking saturation into account has been presented. Mathematical models of an induction motor as influenced by magnetic saturation and saturated indirect vector controller have been presented. The modified model reference adaptive system has been used to estimate the rotor resistance for compensating the rotor resistance variation effect in the vector controlled induction motor performance. The rotor resistance estimation algorithm requires the knowledge of magnetizing

inductance which varies with saturation level in the machine. For this reason, the algorithm has been modified with an online magnetizing inductance estimator. The rotor speed can be synthesized from the induction motor state equations. Digital simulations have been carried out in order to demonstrate the correctness of the proposed drive system. It is concluded that the consideration of magnetic saturation in the dynamic model of the machine and the control part of the system conform with a real simulation of the drive system.

2. DYNAMIC MODEL OF INDUCTION MOTOR AS INFLUENCED BY MAGNETIC CIRCUIT SATURATION

To accommodate the effect of magnetic-circuit saturation, the dynamic model of the induction motor in the stationary $d^s - q^s$ reference frame [13]-[15] has been modified to include the saturation of the main flux path as follows:

$$\frac{di_{ds}^s}{dt} = \frac{1}{L_{ds}}\left[V_{ds}^s - R_s i_{ds}^s - L_{2s}\frac{di_{qs}^s}{dt} - L_{dm}\frac{di_{dr}^s}{dt} - L_{2s}\frac{di_{qr}^s}{dt}\right] \tag{1}$$

$$\frac{di_{qs}^s}{dt} = \frac{1}{L_{qs}}\left[V_{qs}^s - L_{2s}\frac{di_{ds}^s}{dt} - R_s i_{qs}^s - L_{2s}\frac{di_{dr}^s}{dt} - L_{qm}\frac{di_{qr}^s}{dt}\right] \tag{2}$$

$$\frac{di_{dr}^s}{dt} = \frac{1}{L_{dr}}\left[-L_{dm}\frac{di_{ds}^s}{dt} - \left(L_{2s}\frac{d}{dt} + \omega_r L_m\right)i_{qs}^s - R_r i_{dr}^s - \left(L_{2s}\frac{d}{dt} + \omega_r L_{dr}\right)i_{qr}^s\right] \tag{3}$$

$$\frac{di_{qr}^s}{dt} = \frac{1}{L_{qr}}\left[-\left(L_{2s}\frac{d}{dt} - \omega_r L_m\right)i_{ds}^s - L_{qm}\frac{di_{qs}^s}{dt} - \left(L_{2s}\frac{d}{dt} - \omega_r L_{qr}\right)i_{dr}^s - R_r i_{qr}^s\right] \tag{4}$$

The stator and rotor mutual inductance in the d-and q- axes in the above equations are expressed as:

$$L_{dm} = L_0 + L_{2c}, \quad L_{qm} = L_0 - L_{2c}$$

The stator and rotor self inductances in the d- and q-axes are defined in equations (1)-(4) by:

$$L_{ds} = L_{ls} + L_{dm}, \; L_{dr} = L_{lr} + L_{dm}$$

$$L_{qs} = L_{ls} + L_{qm}, \; L_{qr} = L_{lr} + L_{qm}$$

Where

$$L_{2c} = L_2\cos(2\mu), \; L_{2s} = L_2\sin(2\mu)$$

$$L_0 = \frac{L + L_m}{2}, \; L_2 = \frac{L - L_m}{2}$$

$L = d|\lambda_m| / d|i_m|$ is a dynamic mutual inductance equal to the first derivative of the magnetization curve. $L_m = |\lambda_m| / |i_m|$ is a static mutual inductance and can be

also obtained directly from the magnetization curve. Evidently both L and L_m take account of the fact that i_m is continuously changing in time. And μ is the angle of the magnetizing current space vector with respect to the reference axis.
The electromagnetic torque can be expressed as:

$$T_e = \frac{3}{2}\frac{P}{2} L_m \left(i_{qs}^s i_{dr}^s - i_{ds}^s i_{qr}^s \right) \tag{5}$$

The equation of the motion is:

$$J\frac{d\omega_r}{dt} + f_d \omega_r + T_l = T_e \tag{6}$$

Where J is the inertia of the rotating parts, f_d is the damping coefficient of the load and T_l is the shaft load torque. The state form of equation (6) can be written as:

$$\frac{d\omega_r}{dt} = \frac{T_e - f_d \omega_r - T_L}{J} \tag{7}$$

Thus the dependent variables of the system are i_{ds}^s, i_{qs}^s, i_{dr}^s, i_{qr}^s and ω_r. The derivatives of these variables are functions of the variables themselves, motor parameters and stator supply voltage. Simultaneous integration of equations (1)-(5) and (7) predicts the temporal variation of these variables.

3- SATURATED INDIRECT VECTOR CONTROLLER OF THE INDUCTION MOTOR

The estimation of rotor flux value and its phase angle is performed in rotor flux oriented $d^e - q^e$ synchronously rotating reference frame based on stator currents and speed measurement. The rotor flux calculator is derived in such a way that nonlinear relationship between the main flux and magnetizing current is taken into account. In this calculation, the field orientation is maintained, the condition $\lambda_{qr} = 0$ is satisfied, the influence of q-axis magnetizing flux on resultant magnetizing flux can be neglected ($\lambda_{qm} = 0$).
The approximate saturated rotor flux calculator is given with:

$$\lambda_{dm} = \frac{L_{lr}}{R_r}\frac{d\lambda_r}{dt} + \lambda_r \tag{8}$$

$$\omega_{sl} = \frac{L_m}{T_r}\frac{i_{qs}^e}{\lambda_r} \tag{9}$$

$$\lambda_{dm} = \lambda_r + L_{lr}\left[i_{ds}^e - i_{dm}(\lambda_m) \right] \tag{10}$$

$$T_e = \frac{3}{4} P \frac{L_m}{L_r} i_{qs}^e \lambda_r \tag{11}$$

Simplified saturated indirect vector controller can be constructed as shown in Fig. 1 the scheme is described with the following equations:

$$\lambda_m \approx \lambda_{dm} = \frac{L_{lr}}{R_r}\frac{d\lambda_r^*}{dt} + \lambda_r^* \tag{12}$$

$$i_{ds}^{e*} = i_{dm}(\lambda_m) + \frac{1}{R_r}\frac{d\lambda_r^*}{dt} \tag{13}$$

$$i_{qs}^{e*} = \frac{4}{3P}\frac{(L_{lr}+L_m)}{L_m}\frac{T_e^*}{\lambda_r^*} \tag{14}$$

$$\omega_{sl}^* = \frac{L_m}{T_r}\frac{i_{qs}^{e*}}{\lambda_r^*} \tag{15}$$

$$\theta_e^* = \int(\omega_r + \omega_{sl}^*)dt \tag{16}$$

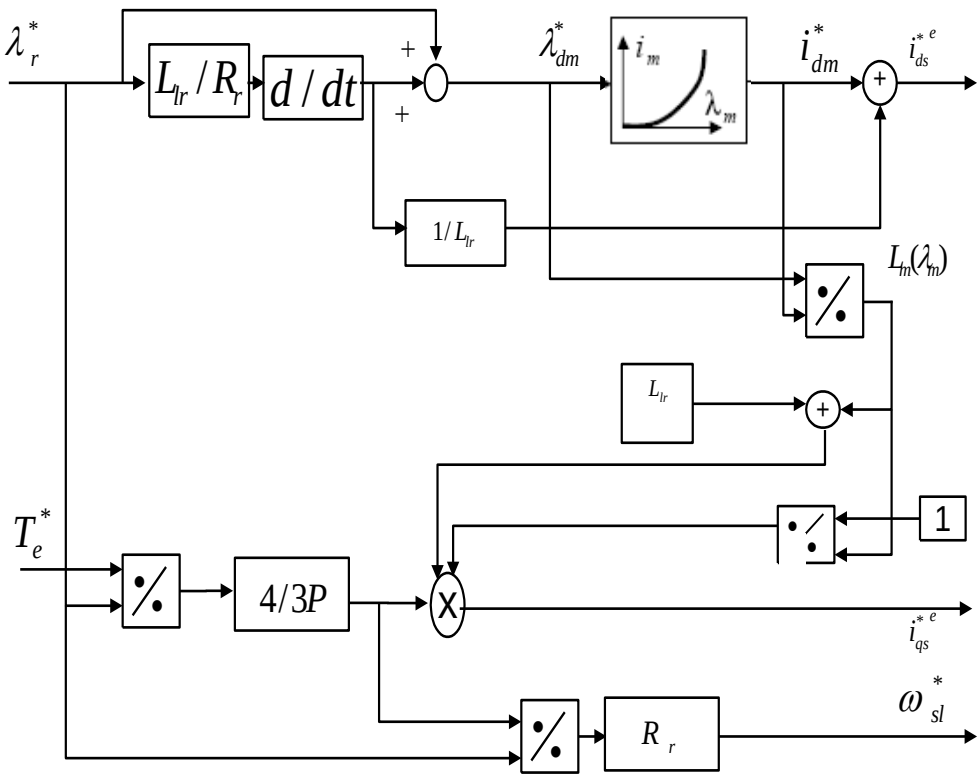

Figure 1: Saturated indirect vector controller scheme

4- ROTOR RESISTANCE IDENTIFICATION BASED ON MRAS

The calculation of slip speed in the indirect method depends on the rotor resistance which changes significantly with temperature and frequency. An error in the slip speed

calculation gives an error in the rotor flux position, resulting in coupling between the flux and torque and hence producing currents due to axis misalignment. This will result in a torque response which possibly overshoot and undershoot and a steady state error is produced. To allow correct estimation of slip speed and consequently proper operation of the sensorless control, it is required to estimate the rotor resistance value. The rotor resistance variation is estimated based on the MRAS technique from the terminals voltages and currents measurements. In order to obtain an accurate estimation of rotor resistance, it is necessary to base the estimation on the coupled circuit equations of the motor. Equations for an induction motor in the stationary $d^s - q^s$ reference frame can be expressed as:

Voltage model (stator equation):

$$p\begin{bmatrix} \lambda_{dr}^{s} \\ \lambda_{qr}^{s} \end{bmatrix} = \frac{(L_m + L_{lr})}{L_m}\left(\begin{bmatrix} V_{ds}^{s} \\ V_{qs}^{s} \end{bmatrix} - \begin{bmatrix} R_s + \sigma L_s & 0 \\ 0 & R_s + \sigma (L_m + L_{ls}) \end{bmatrix}\begin{bmatrix} i_{ds}^{s} \\ i_{qs}^{s} \end{bmatrix}\right) \tag{17}$$

Current model (rotor equation):

$$p\begin{bmatrix} \lambda_{dr}^{s} \\ \lambda_{qr}^{s} \end{bmatrix} = \begin{bmatrix} -\frac{R_r}{L_r} & -\omega_r \\ \omega_r & -\frac{R_r}{L_r} \end{bmatrix}\begin{bmatrix} \lambda_{dr}^{s} \\ \lambda_{qr}^{s} \end{bmatrix} + \frac{L_m}{T_r}\begin{bmatrix} i_{ds}^{s} \\ i_{qs}^{s} \end{bmatrix} \tag{18}$$

Figure 2 indicates an alternative way of estimating the rotor resistance by using the MRAS techniques. Two independent observers are constructed to estimate the components of rotor flux vector, one based on equation (17) and the other based on equation (18). Since (17) does not involve the quantity R_r, this observer may be regarded as a reference model of the induction motor, and (18) which dose involve R_r, may be regarded as an adjustable model. The error between the states of the two models is then used to drive a suitable adaptation mechanism which generates the estimate rotor resistance R_r for the adjustable model until good tracking of the estimated rotor resistance to actual one is achieved. For the purpose of deriving an adaptation mechanism, the rotor resistance is initially treated as a constant parameter of the reference model. Subtracting (18) for the adjustable model from the corresponding equations for the reference model, the following state error equation can be obtained:

$$p\begin{bmatrix} \varepsilon_d \\ \varepsilon_q \end{bmatrix} = \begin{bmatrix} -\frac{R_r}{L_r} & -\omega_r \\ \omega_r & -\frac{R_r}{L_r} \end{bmatrix}\begin{bmatrix} \varepsilon_d \\ \varepsilon_q \end{bmatrix} + \frac{1}{L_r}\begin{bmatrix} \hat{\lambda}_{dr}^{s} - L_m i_{ds}^{s} \\ \hat{\lambda}_{qr}^{s} - L_m i_{qs}^{s} \end{bmatrix}\left[\hat{R}_r - R_r\right] \tag{19}$$

where:

$$\varepsilon_d = \lambda_{dr}^{s} - \hat{\lambda}_{dr}^{s}, \quad \varepsilon_q = \lambda_{qr}^{s} - \hat{\lambda}_{qr}^{s}$$

More ever, equation (19) can be represented in the form:

$$p[\varepsilon] = [A]\cdot[\varepsilon] - [W] \tag{20}$$

Since $\hat{R}_r$ is a function of the state error, these equations describe a non-linear feedback system as indicated in Fig. 3. The hyperstability is assured provided that the linear time-invariant forward-path matrix is strictly positive real and that the nonlinear feedback (which includes the adaptation mechanism) satisfies Popov's criterion for hyperstability [19]. Popov's criterion requires a finite negative limit on the input/output inner product of the feedback system. Satisfying this criterion leads to a candidate adaptation mechanism as follows:

Let $$\hat{R}_r = \left[K_P + \frac{K_I}{p}\right]\phi(\varepsilon) \tag{21}$$

Popov's criterion require that

$$\int_0^{t_1} [\varepsilon]^T\ [W]\ dt \geq -\gamma^2 \quad \text{For all } t_1 \geq 0 \tag{22}$$

Where γ^2 is a positive constant.

Substituting for $[W]$ and $[\varepsilon]$ in this inequality and using the definition of R_r, Popov's criterion for the present system becomes

$$\int_0^{t_1} \left\{ \begin{bmatrix} \varepsilon_d & \varepsilon_q \end{bmatrix} \left[\begin{bmatrix} \hat{\lambda}_{dr}^s - L_m\, i_{ds}^s \\ \hat{\lambda}_{qr}^s - L_m\, i_{qs}^s \end{bmatrix} \frac{1}{L_r} \left(\hat{R}_r - \left[K_P + \frac{K_I}{p}\right]\phi(\varepsilon) \right) \right] \right\} dt \geq -\gamma^2 \quad \text{For all } t_1 \geq 0 \tag{23}$$

A solution to this inequality can be found through the following relation:

$$\int_0^{t_1} k\left(p.f(t)\right) f(t)\, dt \geq -\frac{1}{2} k.\ f(0)^2,\ \ k > 0 \tag{24}$$

The validity of equation (22) can be verified using inequality equation (23) with an adaptive mechanism equation for rotor resistance identification and can be expressed as:

$$\hat{R}_r = \left[K_P + \frac{K_I}{p}\right]\left(\left(\lambda_{dr}^s - \hat{\lambda}_{dr}^s\right)\left(\hat{\lambda}_{dr}^s - L_m\, i_{ds}^s\right) + \left(\lambda_{qr}^s - \hat{\lambda}_{qr}^s\right)\left(\hat{\lambda}_{qr}^s - L_m\, i_{qs}^s\right)\right) \tag{25}$$

Where K_P and K_I are the parameters of PI controller of an adaptation mechanism.

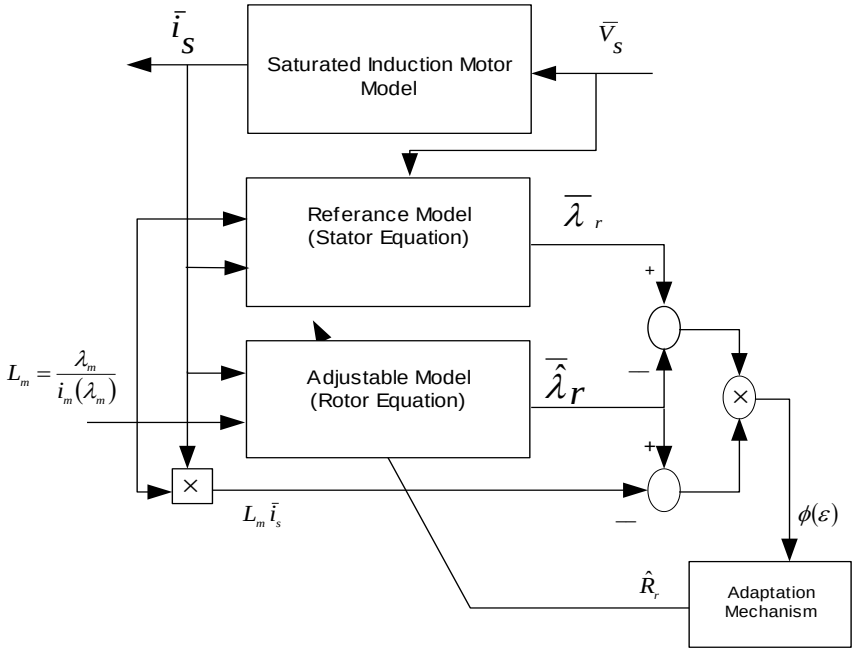

Figure 2: Structure of saturated MRAS system for rotor resistance estimation

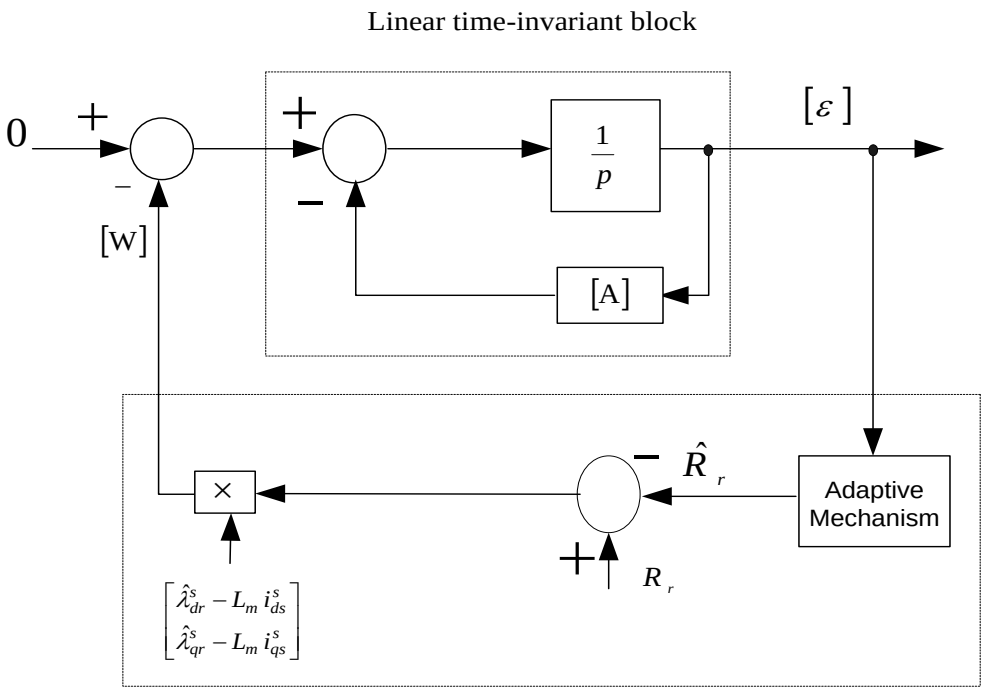

Figure 3: MRAS representation as a nonlinear feedback system

5. ESTIMATION ALGORITHM OF MOTOR SPEED

In vector control schemes, the detection of rotor speed is necessary for calculating the field angle and establishing the outer feedback-loop of speed. Recently, the elimination of speed sensor has been one of the important requirements in vector control schemes because the speed sensor spoils the ruggedness, reliability and simplicity of induction motor drives. Also, the speed sensor can not be mounted in some cases such as motor drives in a hostile environment and high speed motor drives. This is on the expense of adding a speed estimator in the vector control scheme. Given the complete knowledge of the motor parameters, the electrical speed of the rotor flux vector and the instantaneous speed of the motor can be calculated directly.

Firstly, the field angle θ_e of the rotor flux vector λ_r and its derivative are defined as follows:

$$\theta_e = \omega_e t = \tan^{-1} \frac{\lambda_{qr}^s}{\lambda_{dr}^s} \tag{26}$$

$$p\theta_e = \omega_e = \frac{\lambda_{dr}^s \, p\lambda_{qr}^s - \lambda_{qr}^s \, p\lambda_{dr}^s}{{\lambda_{dr}^s}^2 + {\lambda_{qr}^s}^2} \tag{27}$$

From equations (18) and. (27); the rotor speed is estimated by equation:

$$\hat{\omega}_r = \frac{1}{\lambda_r^2}\left[\left(\lambda_{dr}^s \, p\lambda_{qr}^s - \lambda_{qr}^s \, p\lambda_{dr}^s\right) - \frac{L_m}{T_r}\left(\lambda_{dr}^s \, i_{qs}^s - \lambda_{qr}^s \, i_{ds}^s\right)\right] \tag{28}$$

Where

$$\lambda_r^2 = {\lambda_{dr}^s}^2 + {\lambda_{qr}^s}^2$$

From equation (28), it is clear that, the rotor resistance and magnetizing inductance variations have strong influence upon the speed estimation. To estimate motor speed accurately therefore, a rotor resistance estimation algorithm and magnetizing inductance estimation are necessary to compensate the thermal variation in the rotor resistance and to compensate the effect of magnetic saturation.

6- ONLINE IDENTIFICATION ALGORITHM OF MAGNETIZING INDUCTANCE

The accuracy of rotor resistance and speed estimations depend on the precise magnetizing inductance which varies due to the main flux saturation. Magnetizing inductance of an induction motor may vary significantly when the main magnetic flux is saturated. Standard assumption of constant magnetizing inductance is no longer valid and it becomes necessary to compensate for the nonlinear magnetizing inductance variation. Therefore, the structure of the rotor resistance and speed estimators should be modified in such a way that the variation of main flux saturation is recognized within the rotor resistance and speed estimation algorithms. This requires online identification algorithm of the magnetizing inductance.

The magnitude of magnetic flux vector is calculated from their components as:

$$\lambda_m = \sqrt{\lambda_{dm}^{s\ 2} + \lambda_{qm}^{s\ 2}} \tag{29}$$

The air-gap magnetizing flux components can be obtained in the stationary reference frame [11] as:

$$\lambda_{dm}^s = \int (V_{ds}^s - R_s i_{ds}^s)\, dt - L_{ls} i_{ds}^s \tag{30}$$

$$\lambda_{qm}^s = \int (V_{qs}^s - R_s i_{qs}^s) dt - L_{ls} i_{qs}^s \tag{31}$$

The magnetizing curve of the machine is identified offline in the laboratory from no-load test and is represented with a suitable polynomial relating the magnetizing flux with the magnetizing current. Since the magnetizing flux is known, it is possible to estimate the magnetizing inductance using the known non linear inverse magnetizing curve.

$$i_m = f(\lambda_m) \tag{32}$$

$$\hat{L}_m = \frac{\lambda_m(i_m)}{i_m} \tag{33}$$

7- PROPOSED SENSORLESS VECTOR CONTROLLED INDUCTION MOTOR DRIVE

Figure 4 shows the block diagram of the proposed sensorless indirect vector controlled induction motor drive taking saturation into account. It consists mainly of a loaded induction motor model taking saturation into account, a hysteresis current-controlled PWM (CCPWM) inverter, a saturated vector control scheme followed by a coordinate transformation (CT) and an outer speed loop. In addition to the machine and inverter the system include speed controller, an adaptive rotor resistance and motor speed estimators. To compensate the effect of nonlinear magnetizing inductance due to saturation in the accuracy of rotor resistance and rotor speed estimation, an online magnetizing inductance estimator has been constructed and used within the rotor resistance and rotor speed estimators. The magnetizing inductance is estimated based on the measured stator voltages and currents and the inverse magnetizing curve of the machine. The speed controller generates the command q^e – components of stator current $i_{qs}^{*\ e}$ from the speed error between the estimated motor speed and the command speed. The rotor flux reference decreases in inverse proportion to the speed of rotation in the field weakening region, while it is constant and equal to rated rotor flux λ_m in the base speed region and is used to feed the saturated vector controller scheme for obtaining the command of stator current $i_{ds}^{*\ e}$.

Measurements of two stator phase voltages and currents are transformed to d^s - and q^s – components and used in the adaptive rotor resistance, speed and online magnetizing estimators. The coordinate transformation (CT) in Fig. 4 is used to transform the stator currents components command ($i_{qs}^{*\ e}$ and $i_{ds}^{*\ e}$) to the three phase

stator current command (i_{as}^*, i_{bs}^* and i_{cs}^*) by using the field angle θ_e^*. The hysteresis current control compares the stator current to the actual currents of the machine and switches the inverter transistors in such a way that commanded currents are obtained.

8- SIMULATION RESULTS AND DISCUSSIONS

Computer simulations have been carried out in order to validate the effectiveness of the proposed scheme of Fig. 4. The Matlab / Simulink software package has been used for this purpose.

The induction motor under study is a 3.8 HP, four poles motor, its nominal parameters and specifications are listed in table 1. The actual value of the magnetizing inductance in the motor model is considered to account for the magnetic circuit saturation as measured in the laboratory. It is represented as a function of the magnetizing current I_m by a suitable polynomial in the Appendix I.

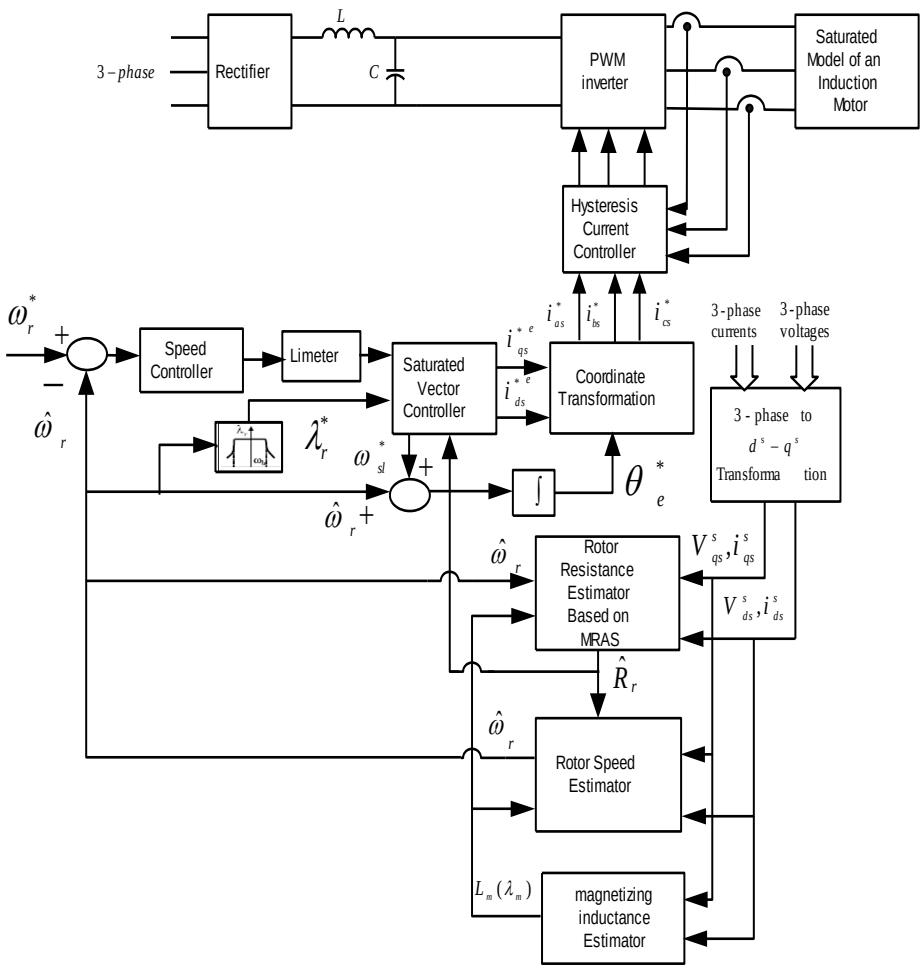

Figure 4: Overall block diagram of the proposed sensorless vector controlled induction motor drive

Table 1: Parameters and data specifications of the induction motor

Rated power (HP)	3.8	Rated voltage (V)	380
Rated current (A)	8	Rated frequency (Hz)	50
Rs (Ω)	1.725	Rr (Ω)	1.009
Ls (H)	0.1473	Lr (H)	0.1473
Lm (H)	0.1271	Rated rotor flux, (wb)	0.735
J (kg.m^2)	0.0400	Rated speed (rpm)	1450

The speed controller parameters are tuned as to give satisfactory speed response when electrical machine parameter errors are absent.

The transient performance of the sensorless drive system is investigated for step change of the rotor resistance when the motor is running at 100 rpm with nominal load torque. Figure 5a, 5b, 5c and 5d show the vector control response when the rotor resistance is increased by 50 % from its nominal value at t = 6 sec. From figures 5b, 5c and 5d, it seen that the estimated motor speed, motor torque and $d^e - q^e$ axes rotor flux components are oscillating and deviate from their command values during the rotor resistance variation. These deviations and oscillations may cause the vector control drive system to become unstable.

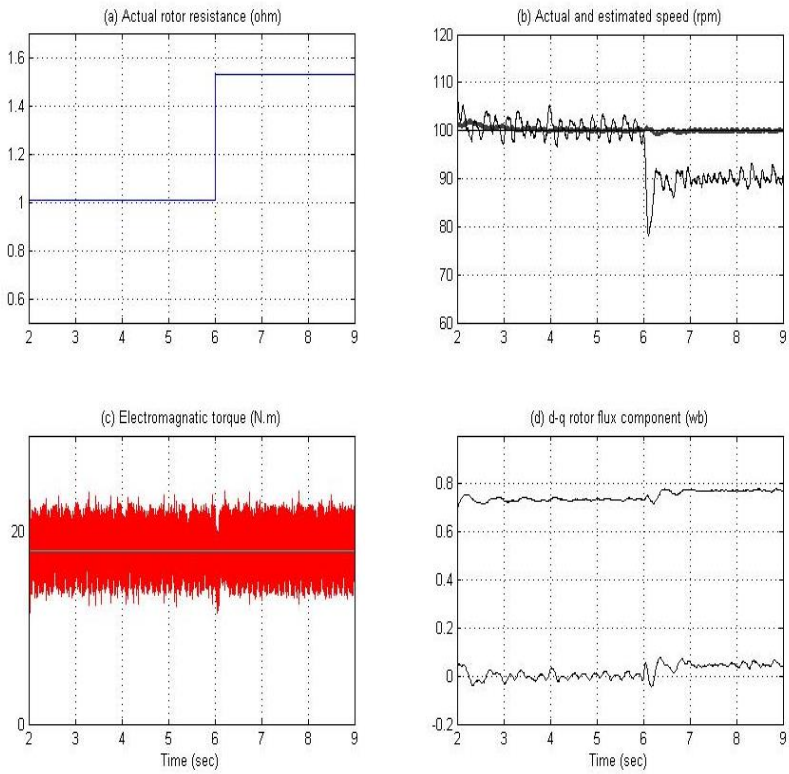

Figure 5: Effect of rotor resistance variation on the motor drive performance.
(a) step variation of rotor resistance, (b) actual and estimated speed,
(c) electromagnetic torque, (d) $d^e - q^e$ axes rotor flux components, and

In order to improve the drive performance, the rotor resistance estimation scheme is introduced with the control system. The estimated rotor resistance is able to track the change in rotor resistance adequately as shown in Fig. 6a. Also, the estimated rotor resistance converges and tracks its actual value after a short delay time. With rotor resistance estimator, the motor torque, estimated speed and $d^e - q^e$ axes rotor flux components are kept constant and matched with their commands as shown in figures 6b, 6c and 6d.

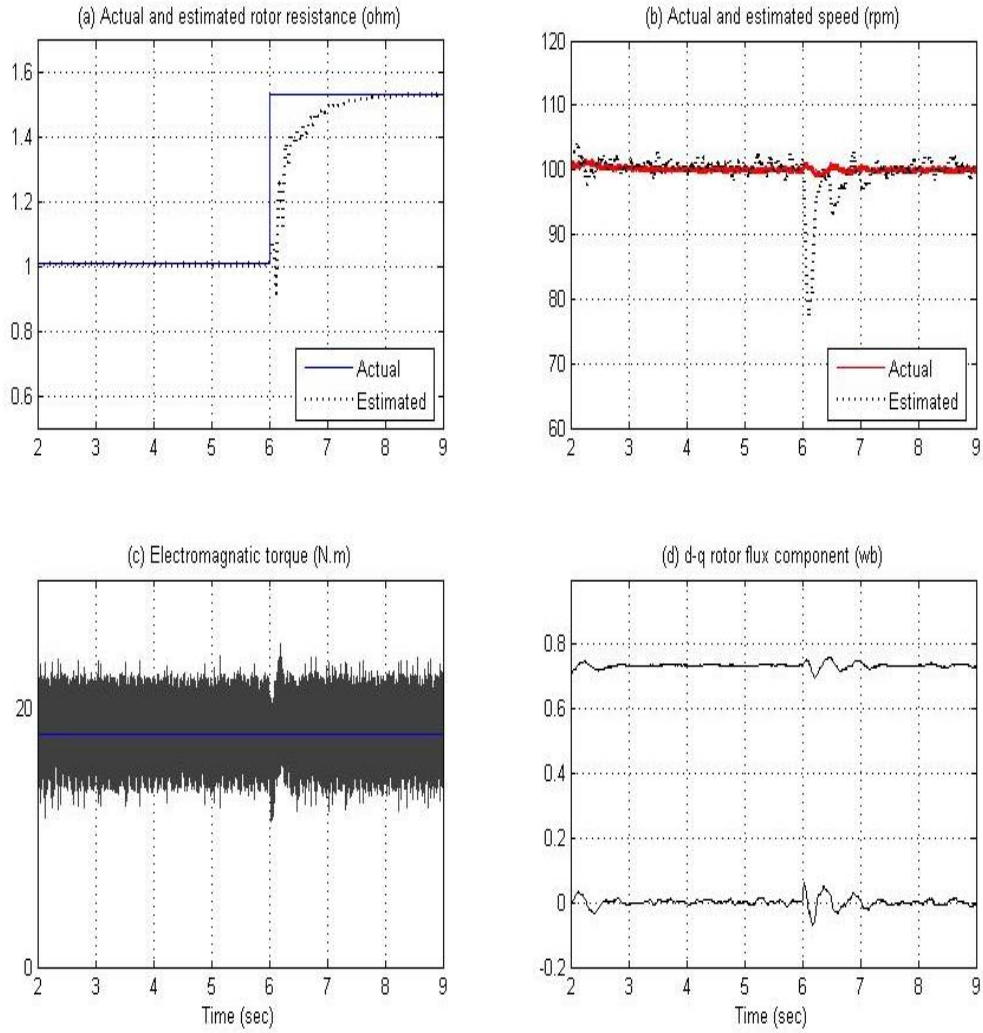

Figure 6: Motor drive performance with the proposed online rotor resistance estimation. (a) actual and estimated rotor resistance, (b) actual and estimated speed, (c) electromagnetic torque and (d) $d^e - q^e$ axes rotor flux components.

The transient performance of the proposed sensorless drive system is investigated for step-change of the load torque when the actual rotor resistance becomes 150 % from its nominal value. Figures 7a, 7b, 7c and 7d show the actual and

estimated rotor resistance, motor speed, electromagnetic torque and $d^e - q^e$ axes rotor flux components, when the motor is subjected to a load disturbance from 10 to 20 N.m (about rated torque) at 100 rpm. Figure 7b shows the dip and overshoot of the estimated motor speed following the application and removal of the load torque disturbance. The speed dip and overshoot are determined by the gains of the speed controller of motor speed loop, as indicated in Fig. 7b. Figure 7c shows fast and good response of the motor torque. However, this torque exhibits high-frequency pulsations of large magnitude due to voltage source inverter pulse width modulation. The rotor flux components are unchanged during the load disturbance as shown in Fig. 7d. This proves that the decoupled control of the torque producing current from the magnetizing current is evident at low speed.

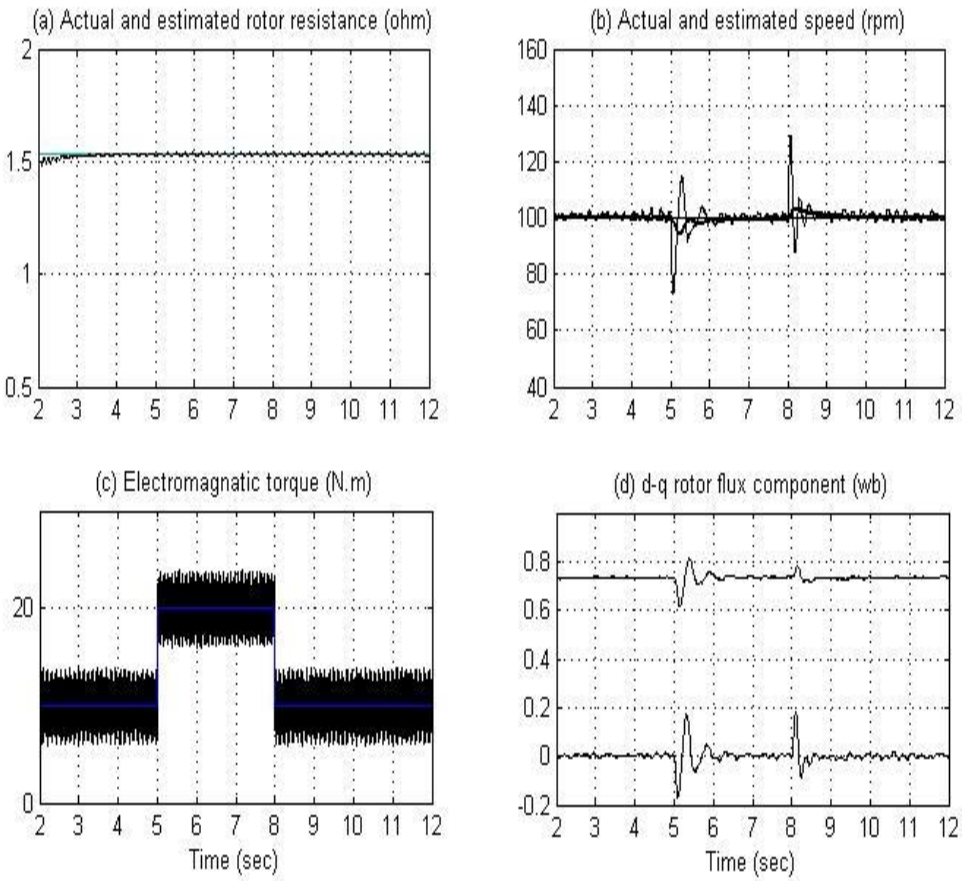

Figure 7: Performance of the proposed sensorless drive system for load torque disturbance. (a) actual and estimated rotor resistance, (b) actual and estimated speed, (c) electromagnetic torque and (d) $d^e - q^e$ axes rotor flux components.

The transient performance of the proposed sensorless drive system is investigated for operation in the field weakening region and the actual rotor resistance is increased by 50 % from its nominal value in step manner at t= 6 second. Figures 8a,

8b, 8c and 8d show the actual and estimated rotor resistance, motor speed, electromagnetic torque and $d^e - q^e$ axes rotor flux components, when the motor speed command changed from 1500 rpm to 1750 rpm in step change fashion at t = 8 second. The rotor flux command decreases in inverse proportion to the speed of rotation in the field weakening region, while it is constant and equal to its rated value in the range of rated speed. The estimated rotor resistance is converged adequately to its actual value after a short delay as shown in Fig. 8a. Figure 8b shows that, the actual and estimate speed have the same track in the field weakening region. The motor torque response exhibits high-oscillations during transient operation and is readjusted to original value after a short delay as shown in Fig. 8c. The rotor flux components agree with their command values during the field weakening region as shown in Fig. 8d. This proves that the decoupled control of the torque producing current from the magnetizing current is evident at speed higher than rated speed.

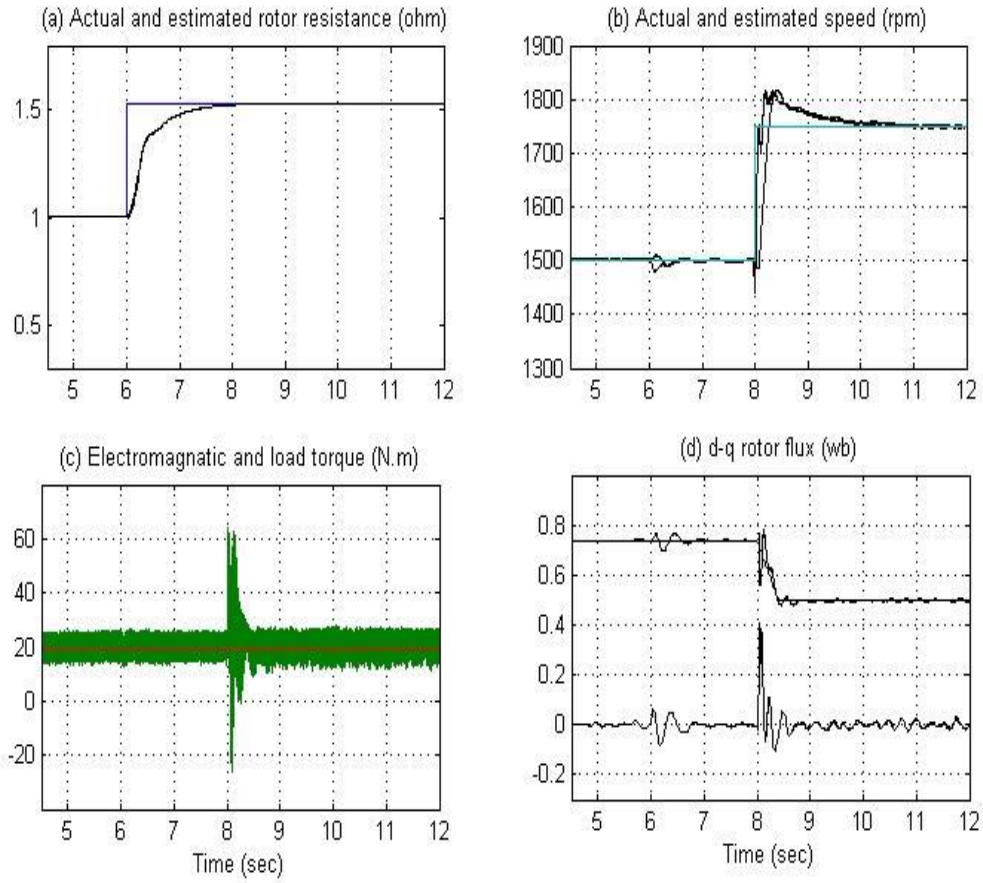

Figure 8: Performance of the proposed sensorless drive system for operation in the field weakening region. (a) actual and estimated rotor resistance, (b) actual and estimated speed, (c) electromagnetic torque and (d) $d^e - q^e$ axes rotor flux components.

Figure 9 shows the variation of the estimated motor speed with various load torque. From this figure, the estimated rotor speed is kept constant during the load torque disturbance. Therefore, the speed estimator is robust against rotor parameter variations in a wide range of motor speed.

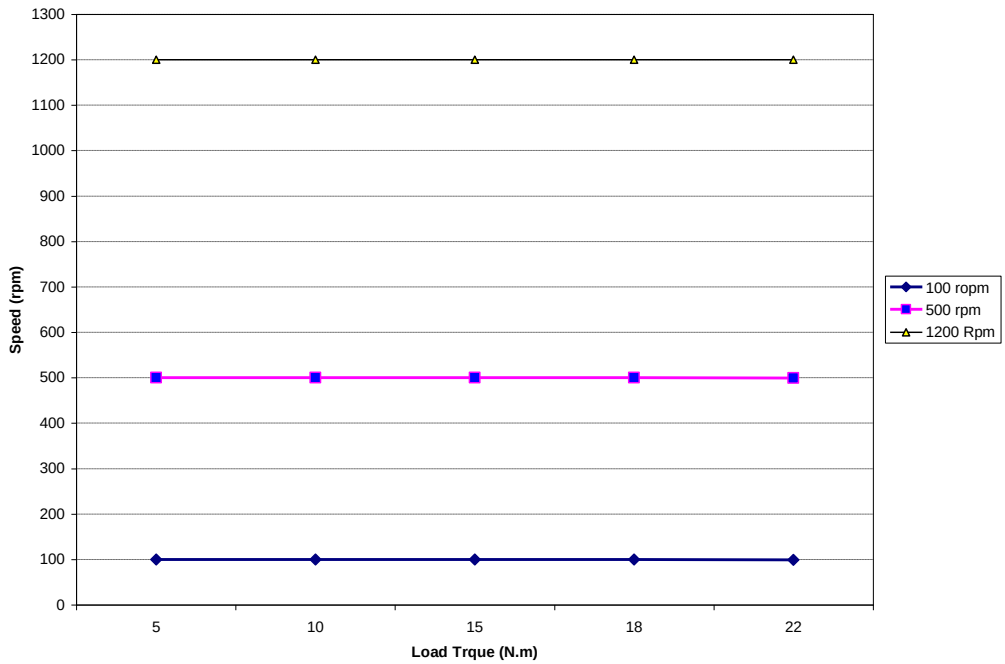

Figure 9: The speed variation with change the load torque

9- CONCLUSIONS

This paper investigates the rotor resistance estimation for speed sensorless controlled induction motor drive system based on the model reference adaptive system technique taking magnetic saturation into account. An effective on-line estimation method for rotor resistance and magnetizing inductance has been proposed to improve the drive performance. The superiority of the modified MRAS over the constant parameter one for operation with saturated main flux or in the field weakening region has been proved. Simulations results are provided to demonstrate smooth steady state operation and high dynamic performance of the proposed drive system in a wide range of motor speed. The main conclusions that can be inferred from the results are summarized as follows:

1. The variation of rotor resistance degrades the performance of the sensorless drive by introducing errors, in the estimated motor speed, motor torque and $d^e - q^e$ axes rotor flux components.
2. The adaptive rotor resistance estimation scheme is capable of tracking the rotor resistance variation very well. It is also seen that the compensator can overcome the problems of instability caused by a large mismatch between the estimated performance and their commands.

3. The transient performance of the proposed sensorless drive is presented when the motor is subjected to a load torque disturbance. The estimated speed response gives a desired dynamic performance which is not affected by the load torque disturbance and the variation of motor parameters. Fast and good response of the motor torque disturbance is achieved following the application and removal of load torque disturbance, this in addition to rotor flux components which are kept constant during the load disturbance.
4. Good and stable operation during field weakening under full load torque is obtained by the proposed sensorless drive system.
5. The estimation of the motor speed and rotor resistance simultaneously results in accurate speed estimation and good performances are obtained after the estimated rotor resistance converges and tracks to its actual values. Consideration of magnetic saturation in the dynamic model of the machine and controller with rotor resistance estimation scheme serve to make the motor control accurate. Therefore, the proposed sensorless drive is robust against the motor parameter variations.

Appendix I

The non-linear relationship between the air-gap voltage and the magnetizing current was measured from no-load test of the induction motor neglecting core losses. Then, the relationship between the magnetic flux and the magnetizing current (i.e. magnetizing curve) has been obtained. The data of the magnetizing curve was fitted by a suitable polynomial which is expressed as:

$$\lambda_{\mathrm{m}} = 0.00001 I_{\mathrm{m}}^{6} - 0.0004 I_{\mathrm{m}}^{5} + 0.0058 I_{\mathrm{m}}^{4} - 0.037 I_{\mathrm{m}}^{3} + 0.082 I_{\mathrm{m}}^{2} + 0.15 I_{\mathrm{m}} + 0.0029$$

The static magnetizing inductance L_m is calculated from the above polynomial as $L_m = \lambda_m(I_m)/I_m$ and the dynamic magnetizing inductance L is calculated from the first derivative of this polynomial as $L = d\lambda_m(I_m)/dI_m$. Figure Appendix I shows the relationship between the magnetizing flux and the magnetizing current.

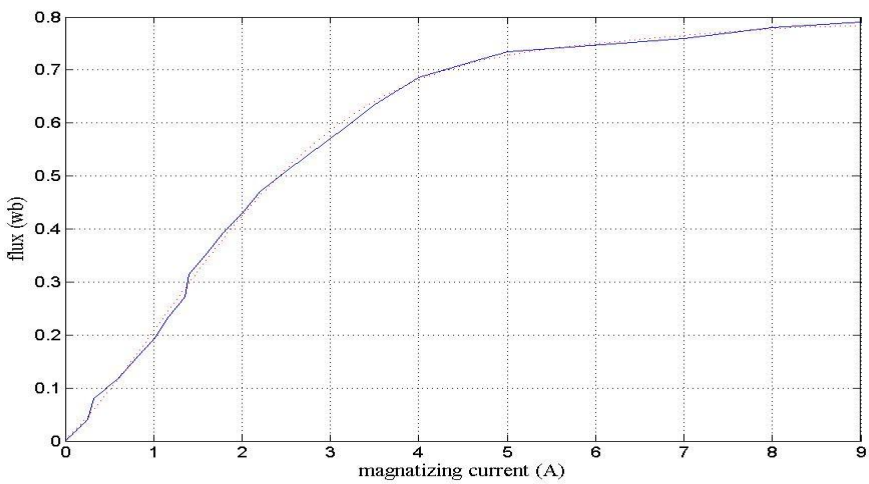

Figure App. I: Magnetizing curve of the induction machine used in simulation.

10- REFERENCES

[1] B. Karanayil, M.F. Rahman and C. Grantham, “Rotor Resistance Identification using Artificial Neural Networks for an Indirect Vector Controlled Induction Motor Drive”, Proc. of the 27 th Annu. Conf. of Industrial Electronics Society, IECON2001, Nov 29 – Dec 2, Denver, USA, Vol. 2, pp. 1315-1320.

[2] Roncero-Sa´ nchez, P., et al., "Rotor-resistance estimation for induction machines with indirect-field orientation.", Control Engineering Practice (2007), doi:10.1016/j.conengprac.2007.01.006 .

[3] R. Marino, S. Percsada, and P. Valigi, “Adaptive input-output linearizing control of induction motors,” IEEE Trans. Automatic Control, vo1.38, pp.208-221, Fcb. 1993.

[4] T.Matsuo, T.A.Lipo, “A rotor parameter identification sachem for vector controlled induction motor drives,” IEEE Trans. on Ind. Appilcal., vol.21, pp. 624-632, May /Junc 1985.

[5] Barut M, Bogosyan OS, Gokasan M., "Switching EKF technique for rotor and stator resistance estimation in speed sensorless control of IMs" Energy Conversion and Management (Elsevier), 48 (2007):3120–3134.

[6] Scott Wade, Matthew W. Dunnigan, and Barry W. Williams, "Modeling and Simulation of Induction Machine Vector Control with Rotor Resistance Identification", IEEE Trans. on power electronics, vol. 12, NO. 3, MAY 1997, pp. 495-50.

[7] H.A.Toliyat, E.Levi, M.Raina; "A review of RFO induction motor parameter estimation techniques", IEEE Trans. on Energy Conversion, vol. 18, no. 2, 2003, pp. 271-283.

[8] T. Noguchi, S.Kondo, and I. Dakahashi, “Field-oriented control of an induction motor with robust on-line tuning of its parameters,” IEEE Trans. Ind. Appl., vol. 33, pp. 35–42, Jan. 1997.

[9] J. C. Moreira and T. A. Lipo, “A new method for rotor time constant tuning in indirect field orient control,” in IEEE Conf. PESC’90,VA, June 1990, pp. 573–580.

[10] Emil Levi, Matija Sokola, and Slobodan N. Vukosavic, "A method for magnetizing curve identification in rotor flux oriented induction machines," IEEE Trans. On Energy Conversion, Vol. 15, No. 2, June 2000, pp. 157-162.

[11] Emil Levi, and Mingyu Wang, "Online Identification of the Mutual Inductance for Vector Controlled Induction Motor Drives," IEEE Trans. on Energy Conversion, Vol. 18, No. 2, June 2003, pp. 299-305

[12] C. R. Sullivan, and Seth R. Sanders, "Models for induction machines with magnetic saturation of the main flux path,” IEEE Trans. Ind. Applicat., vol. 31, no. 4, pp. 907-917, 1995.

[13] Hossam A. Abdel Fattah, Kenneth A. Loparo, Hassan M. Emara, “Induction motor control magnetic system performance under Saturation” Proceedings of the American Control Conference, San Diego, California, l June-1999, PP 1668-1672.

[14] E.Levi, S.Vukosavic, V.Vuckovic, "Saturation compensation schemes for vector controlled induction motor drives", IEEE Power Electronics Specialists Conference PESC, San Antonio, TX, 1990, pp. 591-598.

[15] J. E Brown, K. P Kovacs and P. Vas, "A method of including the effect of main flux path saturation in the generalized Equations of Ac machines", IEEE, Trans. Power Appar. and Sys., Vol. PAS 102, no.1, pp. 96-103,1983.
[16] C. Ilas, A. Bettini, L. Ferraris, G. Griva, and F. Profumo, "Comparison of different schemes without shaft sensors for field oriented control drives", IEEE Conf. in the Ind. Electr. (IECON'94), 3 (1994), pp. 1579-1588.
[17] M. S. Zaky, M. M. Khater, H. Yasin, and S. S. Shokralla, A. El-Sabbe, "Speed-sensorless control of induction motor drives (Review Paper)", Engineering Research Journal (ERJ), Faculty of Engineering, Minoufiya University, Egypt, Vol. 30, No. 4, October 2007, PP. 433-444.
[18] M. S. Zaky, M. M. Khater, H. Yasin, and S. S. Shokralla, "Magnetizing inductance identification algorithm for operation of speed-sensorless induction motor drives in the field weakening region", IEEE Conf. MEPCON, Aswan, Egypt, 2008, PP. 103-108.
[19] C. Schauder, “Adaptive speed identification for vector control of induction motor without rotational transducers”, IEEE Trans. Ind. Appl. 28 (5) (1992) 1054–1061.

تقييم مقاومة العضو الدوار في التحكم الاتجاهى للمحرك الحثى بدون حساس سرعة مع أخذ التشبع المغناطيسي في الاعتبار

ملخص– يهدف البحث إلى تقديم طريقة لتقدير مقاومة العضو الدوار للمحرك الحثي لاستخدامها في التحكم الأتجاهى للمحرك بدون استخدام مقياس للسرعة مع الأخذ في الاعتبار تأثير ظاهرة التشبع المغناطيسي في الحديد. وتم تقديم نموذج رياضي للمحرك الحثى أخذاً في الاعتبار ظاهرة التشبع المغناطيسي في الحديد. وعلاوة على ذلك، تم تعديل المحكم الخاص بالتحكم الأتجاهى لكي يحتوي على قيمة المحاثه المغناطيسية المشبعة. وفي هذا النظام، تم تقديم طريقة فعالة لتقدير مقاومة العضو الدوار معتمداً على النموذج المرجعي للنظام الملائم للحصول على دقة عالية للتحكم في السرعة في مدى واسع للتشغيل. وأيضا تم تقييم سرعة المحرك اعتمادا على حساب الفرق بين السرعة التزامنية للمحرك وسرعة الإزاحة. وقد تم أخذ ظاهرة التشبع المغناطيسي في الاعتبار بعمل مقدر لقيمة المحاثه المغناطيسية للعمل مع النظام. وتم عرض نتائج باستخدام الحاسوب لتوضيح مدى قدرة الطريقة المقترحة للتطبيق. وقد برهنت النتائج المعروضة على أن خواص نظام المحرك جيدة في الحالة الديناميكية والاستاتيكية وهذا يؤكد قدرة الطريقة على تحقيق الأغراض المطلوبة.